Soft Material Characterization of the Lamellar Properties of Starch: Smectic Side-Chain Liquid-Crystalline Polymeric Approach

D. R. Daniels* and A. M. Donald

Polymers and Colloids Group, Cavendish Laboratory, University of Cambridge, Madingley Road, Cambridge CB3 0HE, UK

Received June 30, 2003; Revised Manuscript Received December 12, 2003

ABSTRACT: We compare and contrast the soft lamellar material properties of starch with those of a canonical multilayered microemulsion via the modeling of experimentally observed small-angle X-ray scattering (SAXS) patterns. Consequently, and by using a well-known lamellar microemulsion system as a valuable point of reference, model analysis of the SAXS data enables us to quantitatively characterize the lamellar structure of starch for the first time. We argue that this work provides strong evidence for viewing the lamellar structure of starch as a smectic side-chain liquid-crystalline polymer. Pursuing this approach, we are able to shed light on many of the interesting lamellar features of starch found in this work, over and above those found in more familiar smectic systems. We also address, and draw attention to, the possible use of valuable lessons gained from this work in the design and synthesis of novel soft lamellar materials.

Introduction

Soft materials are often characterized by some limited or intermediate degree of ordering in their concomitant self-assembly. Perhaps the most familiar examples of this kind of self-organizing behavior are to be found in lamellar systems, such as canonical smectic liquid crystals[1−4] and amphiphilic membrane multilayers.[5−8] Similar lamellar morphologies are also ubiquitous within the context of side-chain liquid-crystalline polymers.[9−14]

Considerations of assembly in lamellar materials are often governed by the combined effects of packing constraints, connectivity, and mobility of their constituent units (consistent with filling a space). For example, in amphiphilic membrane systems (held together by hydrophobic/hydrophilic interactions), the geometry of the underlying surfactant units is crucial in determining which of a number of equilibrium macroscopic structures is assumed[1,5] (see Figure 1). Furthermore, in side-chain liquid-crystalline polymers,[2,9−14] the combination of connectivity (of the backbone) with that of flexibility (of the spacers) and rigidity (of the mesogens) leads to typically smectic supramolecular assemblies.[9−14] Such lamellar assembly considerations, familiar from soft condensed matter, also arise in the living world[15] and have recently found new relevance within the biological context of the lamellar morphology of starch,[16−19] the topic of this paper.

Starch is made up of glucose polymers and is of huge importance since it forms the major component of most of our staple foods. The structure of starch granules is now understood[16−25] to be organized on many different length scales (see Figure 2). Amylopectin molecules (branched polymers of glucose units ∼0.1 nm) arrange themselves into alternating lamellae (∼10 nm) of rigid, double-helical (mesogenic) units and more flexible, unbranched (spacer) units. These spacer units are also connected to long, flexible linear backbones of amylopectin (see Figure 3). This gives starch the fascinating structure of a naturally occurring side-chain liquid-crystalline polymer (SCLCP).[17−19] A finite number of these lamellae form discrete growth rings[16−25] on the scale of ∼0.1 μm, up to the whole granule morphology at 1−100 μm.

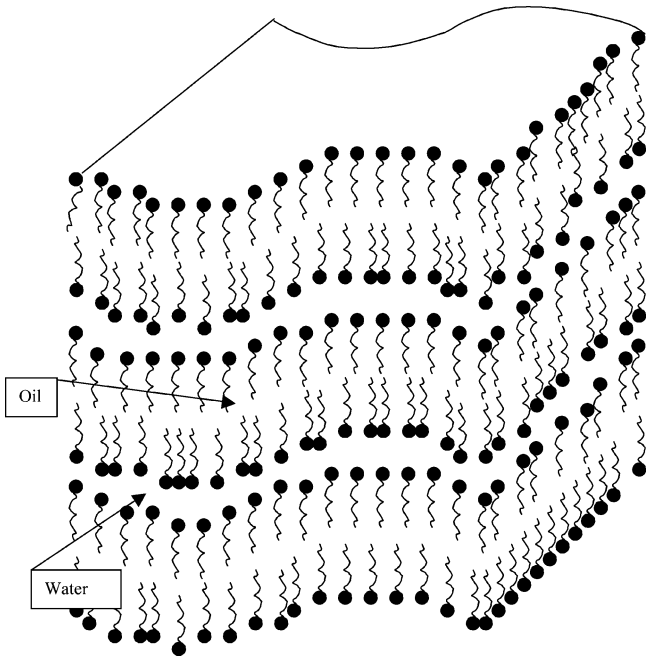

Figure 1. Schematic diagram of model microemulsion packing and lamellar structure.

Starch granules can be further broadly classified as consisting of one of two crystal types called A and B (depending on the local, fine scale crystalline structure at lengths ≤1 nm), which appears to correlate with the total side-chain length.[17−19,26−28] This correlation suggests that B-type starches tend to possess shorter flexible spacers, whereas A-type starches tend to have longer spacer units.[26,28]

Pursuing the SCLCP theme, previous work[17−19] put forward the qualitative idea that given enough freedom (via longer or more flexible spacers), the lamellae in starch ought to arrange themselves into a flat layered structure, with the rigid amylopectin mesogen units

10.1021/ma030360h CCC: $27.50
Published on Web 01/28/2004

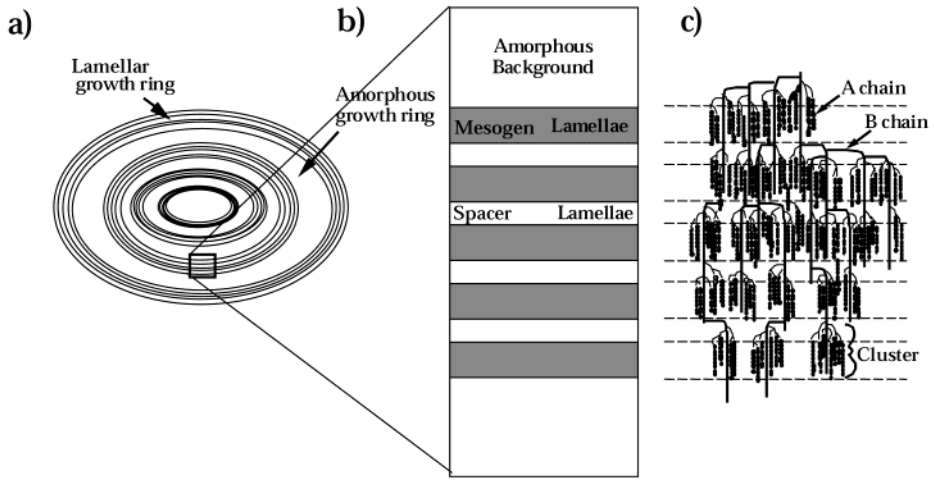

Figure 2. Schematic diagram of starch granule lamellar structure.

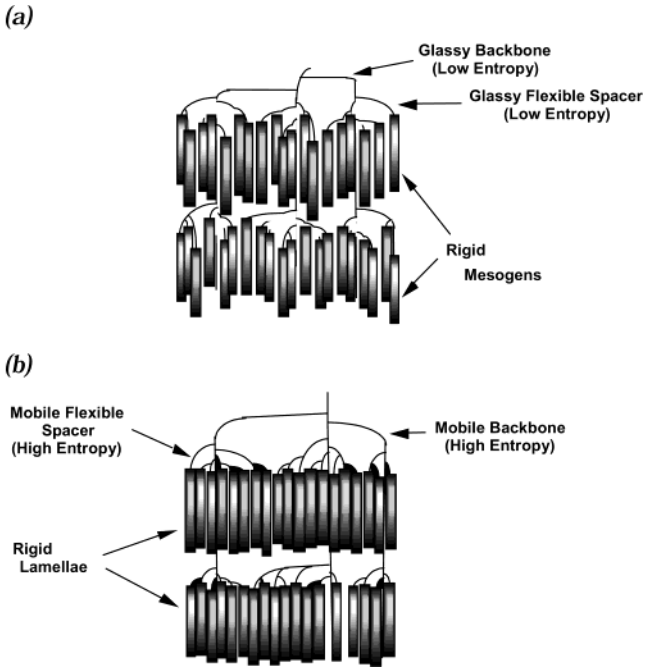

Figure 3. Lamellar structure of a smectic side-chain liquid-crystalline polymer, including a schematic diagram of flexible spacer and rigid mesogen units (a) out of register and (b) in register.

being well-aligned, corresponding roughly to smectic ordering. If this is no longer possible (due to shorter or less flexible spacers), then the lamellae ought to display much greater layer bend and curvature (see Figure 3),[17−19,27] corresponding roughly to nematic ordering.

In this article we will quantitatively view the lamellar structure of starch, as arising from its smectic side-chain liquid-crystalline polymer (SSCLCP) properties. In pursuing this approach, we can draw on a great deal of experimental and theoretical work[9−11] on SCLCPs, where it is indeed found[12−14] that SCLCPs are more frequently found smectic than nematic. The reason for this is straightforward and is due to the antagonistic behavior between aligned, rigid mesogenic groups and the polymer backbone.[12−14] Following on from this, one emphasis of the work to be presented here is that increasing the length of the flexible spacer units (particularly across starch cultivars) leads to a reduction in the coupling of the mesogenic units to the backbone, allowing for far easier formation of smectic layers.[17−19,27] Furthermore, it is typically found in SCLCPs that the glass transition temperature decreases with increasing spacer length,[17−19] with shorter spacers leading to nematic phases and longer spacers leading to smectic phases.

The purpose of the work presented here is to give a quantitative model comparison, and accurate characterization, of the experimentally observed lamellar structure of starch, viewed as a SSCLCP. To highlight and corroborate its interesting lamellar properties, we further compare and contrast the determined smectic structure of starch with that of a representative and much studied amphiphilic multilamellar system[5,6] via the modeling of experimentally obtained SAXS patterns.

Structure, Scattering, and Correlations of Lamellar Materials. We now recap some of the more salient features of lamellar systems relevant to this work, namely the relationship between their structure and scattering properties. It has long been recognized in (thermotropic) smectic liquid crystal[1−4] and (lyotropic) surfactant membrane[29−33] systems that layer bending fluctuations destroy ideal one-dimensional long-range periodic order.[1,2] Both of these systems share the same symmetry class in their structures, which must therefore be necessarily reflected in the universality of the correlations they exhibit.[1,2,5] The absence of long-range order (LRO) in such systems (replaced by what is known as[1] quasi-long-range order (QLRO)) is indeed most easily observed in scattering experiments, with the appearance of characteristic quasi-Bragg-shaped peaks[1−8,29−33] due to layer curvature fluctuations. The absence of long-range order in canonical smectic and membrane systems implies that the mean-square fluctuation in the layer separation diverges logarithmically with the number of layers and that the tails of the scattering peak decay according to characteristic power law line-shaped behavior.[31−33] On the other hand, systems characterized by long-range order possess mean-square fluctuations in the layer separation that diverge linearly with the number of layers, and the scattering peaks display characteristic Gaussian line-shaped behavior.[31−33]

Generally, lamellar systems can undergo two distinct and competing types of fluctuations: those given by layer compression and those given by layer bending. In the limit of very small layer curvature (and therefore very large intralamellar correlation length), the layers become increasingly flatter and smoother. The lamellar

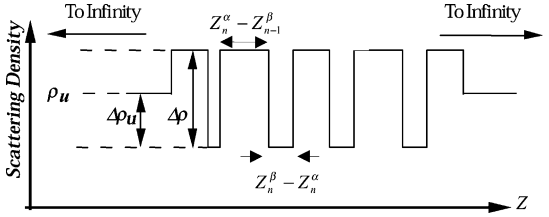

Figure 4. Schematic diagram of scattering electron density profiles for the starch and microemulsion systems studied.

fluctuations are then entirely governed by compression alone (with negligible layer bending) producing Gaussian-like Bragg peaks characteristic of long-range order. This scattering signature is in contrast to the power-law-like Bragg peak signature, characteristic of quasi-long-range order, produced as a result of larger layer curvature fluctuations, expected to be present in typical smectic or lamellar scattering patterns.[1−8]

Model. Modeling of the general lamellar structure of the surfactant-based system and starch samples, studied in this work, was carried out using the following well-known[30−33] free energy, familiar from canonical smectic liquid crystal[2−4] and amphiphilic membrane[5−8] systems:

$$F = \frac{1}{2}\sum_{n=1}^{N}\int \mathrm{d}^2x_\perp [B_\alpha(u_n^\alpha - u_{n-1}^\beta)^2 + B_\beta(u_n^\beta - u_n^\alpha)^2 + K_\alpha(\nabla_\perp^2 u_n^\alpha)^2 + K_\beta(\nabla_\perp^2 u_n^\beta)^2] \quad (1)$$

The terms involving the moduli B_α and B_β represent the compressive fluctuations (along the z-axis, normal to layers) which try to maintain the ideal layer spacing between consecutive layers. The terms involving the moduli K_α and K_β represent the layer curvature fluctuations allowing for individual layer bending. The variables u_n^α and u_n^β in eq 1 describe fluctuations away from the ideal lamellar structure of flat, precisely spaced layers, in which we parametrize our multilayer stack by introducing the following coordinate displacements along the z-axis, Z_n^α and Z_n^β (with origin Z_0), as follows (see Figure 4):

$$Z_n^\alpha = Z_0 + \phi d + (n-1)d + u_n^\alpha$$
$$Z_n^\beta = Z_0 + nd + u_n^\beta \quad (2)$$

Here, ϕ is the fraction of each layer of one component relative to the other component (e.g., mesogen/spacer for starch and oil/water for a microemulsion), and d is the lamellar spacing. The indices α and β are required to keep track of the alternating subregions within one layer repeat distance of our lamellae, given by the mesogen and spacer lamellar components for starch or the oil and water components for the amphiphilic case.

Using the above coordinates, we can write our electron density ρ for N layers as

$$\rho(x,y,z) = \sum_{n=1}^{N}[(\Delta\rho - \Delta\rho_u)(U(z - Z_{n-1}^\beta) - U(z - Z_n^\alpha)) - \Delta\rho_u(U(z - Z_n^\alpha) - U(z - Z_n^\beta))] \quad (3)$$

where $U(z)$ is the unit step function, and $\Delta\rho - \Delta\rho_u$ and $\Delta\rho_u$ refer respectively to the electron densities of the mesogen and spacer regions for starch or the oil and water regions for the amphiphilic case (see Figure 4). Relative electron densities are normalized with respect to a background electron density ρ_u (see Figure 4). Utilizing the Fourier transform, $\rho^*(q)$, the structure factor is given by $S(q) = \rho^*(q)\rho(q)$, with the averaged structure factor $\langle S(q)\rangle$ obtained by taking into account all u_n^α and u_n^β correlations.

By way of an example, we quote here the calculation of a typical correlation average $\langle(u_n^\alpha - u_m^\alpha)^2\rangle$ (where the indices n and m refer to the nth and mth layers of a stack along the z-axis).[27−33]

$$\langle(u_n^\alpha - u_m^\alpha)^2\rangle = \frac{\pi}{4\xi^2}\frac{B_\alpha + B_\beta}{B_\alpha B_\beta}\frac{\xi^2}{\lambda\pi^2}(\ln(1 + \lambda\pi^2|n-m|/\xi^2) + \pi^2(r - r')^2/4\xi^2) \quad (4)$$

All other correlation functions can be similarly obtained straightforwardly via an analogous analysis.[27−33] In the above, we have defined λ through the expression $\lambda^2 = (B_\alpha + B_\beta)(K_\alpha + K_\beta)/B_\alpha B_\beta$ and have introduced the well-known de Gennes−Taupin length[34] for fluctuating surfaces, ξ, as the length scale up to which the layer normal vectors remain correlated.

For ease and clarity of presentation in what follows, we choose to make the following convenient definitions of the parameters in our model of general lamellar deformations:

$$\frac{\pi}{4\xi^2}\frac{1}{B_\alpha} \leftrightarrow (\phi\beta d)^2$$
$$\frac{\pi}{4\xi^2}\frac{1}{B_\beta} \leftrightarrow ((1-\phi)\beta d)^2$$
$$\frac{\lambda\pi^2}{\xi^2} = \epsilon$$
$$\frac{\pi}{8\xi^2\lambda}\left(\frac{1}{B_\alpha} + \frac{1}{B_\beta}\right) = \delta \quad (5)$$

The parameter β gives a measure of layer compression fluctuations, while ϵ and δ give a measure of layer bend and layer splay fluctuations, respectively. Furthermore, β governs the width of the compressional Gaussian layer separation distribution, while ϵ governs the deviation of individual lamellar scattering behavior away from purely Gaussian behavior (as predicted by the compressional fluctuations alone). The parameter δ controls the deviation of lamellar normal alignment away from the preferred direction along the z-axis.

From the above expression for $\langle(u_n^\alpha - u_m^\alpha)^2\rangle$ we can see that typically our structure factor splits into two contributions and can therefore be factorized into longitudinal $\langle S_{\parallel}(q)\rangle$ (parallel to the z-axis, $\parallel$, involving $|n-m|$ alone) and transverse $\langle S_\perp(q)\rangle$ (perpendicular to the z-axis, $\perp$, involving $|r - r'|$ alone) components.[27] In this way we are able to write for the total scattering: $\langle S(q)\rangle = \langle S_{\parallel}(q)\rangle\langle S_\perp(q)\rangle$.

The $\langle S_\perp(q)\rangle$ contribution serves in giving rise to an angular distribution function $P(\vartheta)$, where ϑ is the angle between the layer normal vector and the longitudinal z axis:

$$P(\vartheta) = \frac{1}{C}\,\mathrm{e}^{-(1/\delta)\tan^2\vartheta}/\cos^2\vartheta \quad (6)$$

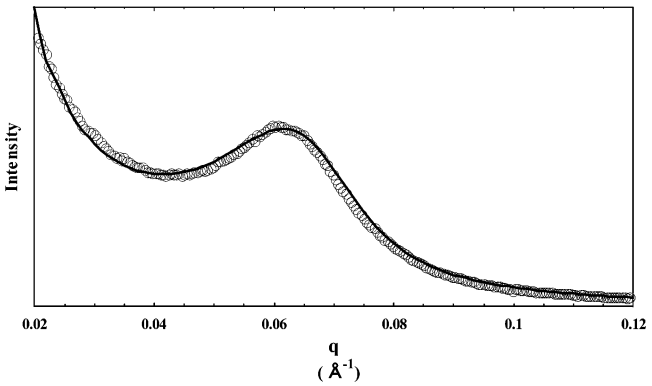

Figure 5. Plot of experimental data (open circles) vs model prediction (solid line) for waxy maize.

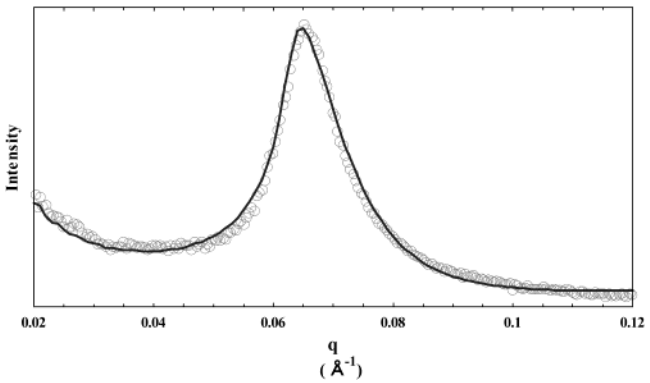

Figure 6. Plot of experimental data (open circles) vs model prediction (solid line) for potato.

with δ as given above, and the constant C is chosen such that $\int_0^\pi d\vartheta \sin\theta P(\vartheta) = 1$. Thus, our final expression for the structure factor $\overline{\langle S(q)\rangle}$ requires an average over all layer normal orientations ϑ using the distribution function $P(\vartheta)$ as follows:

$$\overline{\langle S(q)\rangle} = \frac{1}{4\pi q^2}\int_0^\pi d\vartheta \sin\vartheta P(\vartheta)\langle S_{||}(q\cos\vartheta)\rangle \qquad (7)$$

where $1/4\pi q^2$ is the usual Lorentz factor.[35]

Experimental Methods

Slurries of the different starch species in water were prepared in cells with a typical concentration of 45 wt % starch. At this concentration there was sufficient starch to prevent the suspension sinking within the cell. Scattering experiments were performed at the Synchrotron Radiation Source at Daresbury on beamlines 8.2 and 2.1. The high-intensity beam was collimated with slits and focused on a quadrant detector. The data were normalized, divided by the detector response, and the background scattering (as recorded by a blank sample cell) was subtracted. Changes (further details can be found in refs 16−21) in scattering due to beam damage of the sample were negligible for these experiments. The starches used, waxy maize and potato, were obtained as gifts from National Starch & Chemical Co.

The X-ray scattering data for the model multilayer used in this work were taken with kind permission from ref 6. The microemulsion consisted of the quaternary mixture of sodium dodecyl sulfate (SDS, the surfactant), pentanol (cosurfactant), water, and dodecane. The lamellar phase was made up of water embedded in oil with surfactant at the interface, and there were no electrostatic interactions between layers. In ref 6, SAXS patterns were obtained under various dodecane dilutions, but we choose to quote only the data of the particular case of 54 wt % dodecane, which was most suited for purposes of comparison to our analagous starch SAXS patterns. The mixtures used in ref 6 were contained in sealed quartz capillaries, with diameters of 1 and 2 mm, which yielded randomly oriented lamellar domains (powder averaged). For further details we refer the reader to ref 6.

Results

We now compare and contrast the scattering results obtained for our lamellar samples, as shown in Figures 5−7. Fitting of the model parameters to the experimental data was most easily carried out by eye, with the previous work of refs 16−19 and 27 serving as a useful consistency check. It might be noted here, in passing, that we have chosen for convenience not to display our results in a log−log format, since the range of wave vectors over which, for example, straight-line behavior might feasibly exist is too limited. Besides, all the lamellar samples studied here have also undergone powder averaging, making the reliable extraction of any possible and clean power-law exponents in the observed scattering somewhat problematic.

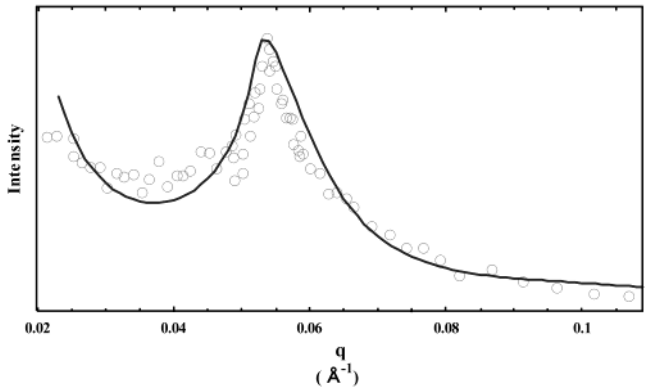

Figure 7. Plot of experimental data (open circles) vs model prediction (solid line) for a model microemulsion (experimental data points taken from ref 6).

Table 1. Model Parameters Used To Fit the Experimental Data

	β	d (nm)	ϕ	N	$\Delta\rho$	$\Delta\rho_u$	ϵ	δ
waxy maize	0.38	8.8	0.65	16	1	0.50	0.01	0.01
potato	0.23	10.0	0.73	20	1	0.80	0.40	0.24
microemulsion	0.28	12.1	0.87	100	1	0.01	0.80	0.30

From Table 1 waxy maize can be seen to be (see also eq 5) the most compressible (higher β, lower compressibility modulus B) of the samples studied, while potato is the most incompressible (lower β, higher compressibility modulus B), with the microemulsion somewhere in between. This implies that the purely compressional fluctuations in our model microemulsion system are somewhat intermediate between those of waxy maize and potato.

Furthermore, we can see from Table 1 that our model microemulsion possesses the highest values of ϵ (bend) and δ (splay) of the samples studied, while waxy maize is characterized by the lowest values of bend (ϵ) and splay (δ), with potato somewhere in between. This implies that our model microemulsion has the largest average layer curvature of all the samples studied and waxy maize the lowest curvature, with potato midway between. This also implies that the lamellae in waxy maize are the most well-aligned along the layer normal, with the microemulsion the least well-aligned and potato somewhere in between.

The value of ϕ for the amphiphilic material gives the ratio of the width of the oil layer to the overall width of the oil and water layer repeat distance, so that we can see that the microemulsion layers consist predominantly of oil. The ϕ values for the starches studied correspond to the relative lengths of the rigid mesogen and the flexible spacer units. From Table 1 we can infer (in tandem with refs 17, 27, 28, and 36) that waxy maize possesses far longer flexible spacer units than potato. The importance and significance of this singular experimental fact will become apparent when, in the following sections, we consider its crucial consequences for the lamellar properties of our studied starches.

The layer spacing d in Table 1 shows some variation between waxy maize and potato. In general, a larger value of δ requires a larger "bare" d value as input into the model, since after allowing for splay fluctuations, governed by δ, the "effective" d actually projected along the z-axis is somewhat less than the initial "bare" d value. Simple trigonometry gives us roughly $\langle d_{\mathrm{eff}} \rangle \approx d_{\mathrm{bare}}(1 - \delta/4)$. This explains why the d value in Table 1 can be higher for potato than that for waxy maize, even though the underlying layer repeat distance may be very similar.

There exists a considerable variation in the values of $\Delta\rho_{\mathrm{u}}$ required for fitting waxy maize and potato starches. Consideration of the $\Delta\rho_{\mathrm{u}}$ values obtained for our samples is problematic, since it is an extremely complicated question as to how the electron density distributions arise in native starches; they are likely to depend on such variables as the amount of water present, A or B crystal type, etc. This was true in all previous work also.[16−19,27] The $\Delta\rho_{\mathrm{u}}$ value for our amphiphilic system can be seen to be negligible from Table 1; however, given the very high value of N for this material, the fit to the experimental data is relatively insensitive to the value of $\Delta\rho_{\mathrm{u}}$ used. We have set $\Delta\rho = 1$ throughout this work, which merely reflects an overall normalization choice for our relative scattering intensities.

The fits from Table 1 are fairly insensitive to the number of layers N, with our model microemulsion possessing a far greater number of lamellae than the starches studied. Such a large N mainly serves to slightly alter the low-q behavior of the SAXS pattern, to the far left of the main peak. Besides, theory[35] consistently predicts a strong $1/q^2$ dependence for the multilamellar scattering intensity at low q. This behavior is indeed observed experimentally for all our samples.

We can also observe immediately from Figures 5−7 notable qualitative differences in the line shapes of the (powder-averaged) experimentally observed scattering patterns across the samples studied. Crudely (yet accurately) put, waxy maize can be seen to exhibit the most rounded experimentally observed scattering maximum of all, while the microemulsion displays the sharpest (or most cusplike) experimentally observed scattering peak, with potato somewhere in between.

The above qualitative considerations, along with the experimental evidence supplied by Table 1, are wholly consistent with the following picture.[1,2,5,9,10] On one hand, our microemulsion is dominated by curvature fluctuations, leading to a more power-law-like (albeit powder-averaged) shape in its scattering peak.[31−33] On the other hand, waxy maize is dominated by compressional fluctuations, leading to a more Gaussian-like shape in its scattering peak,[31−33,35] with potato lying somewhere between these two extremes. Clearly disorder will always tend to broaden any scattering peaks. What is perhaps most interesting here is the difference in the underlying source of disorder present across the samples studied, underscoring the essentially competing effects of curvature and compression.

Discussion

We have studied the lamellar structure of starch granules and a surfactant-based system, via experimentally observed small-angle X-ray scattering patterns, using a model description that has enjoyed enormous success in analogous fluctuating lamellar contexts, such as those found in membrane[5−8,29−33] and smectic liquid crystal systems.[1−4] By careful qualitative and quantitative analysis of the observed scattering behavior (using the model outlined above), we can now characterize effectively the lamellar structure of the starches studied, with reference to that of a well-known, canonical surfactant-based multilayered system.[6]

Comparing and contrasting the results obtained above for the starches used and our model microemulsion,[6] several interesting features emerge. For relatively flat layers (as typified by waxy maize) we see broadened, Gaussian−Bragg peaks dominated by compressional fluctuations alone.[31,32] In the presence of dominant transverse layer fluctuations (as typified by the microemulsion), we get quasi-Bragg peaks, described by well-known power-law-like behavior (albeit powder-averaged).[1−8,31−33] Potato, on the other hand, can be observed to possess a lamellar structure somewhere in between these two extremes and is neither dominated exclusively by layer compression or layer curvature fluctuations.

The work presented here, supported by refs 27 and 28, indicates that starch can be broadly classified into compression or bend/splay dominated categories depending on the length and flexibility of the spacer units.[17−19,26−28] The longer (or less constrained) the flexible spacers, the more easily the mesogens can align and therefore reduce their layer bending while allowing more compressibility. The shorter or less plastic the flexible spacer, the more easily the mesogens can be pulled out of register with one another, leading to more pronounced layer bending and a higher incompressibility. Much characterization work[26−28,36] that has been carried out points to the existence of distinct variations in the lengths of the flexible spacer units across starch species. Indeed, the overwhelming conclusion drawn from the work of refs 26−28 and 36 was that the spacer units in potato starch tended to be significantly shorter than those of waxy maize. In this work, supported by refs 26−28, we indeed find that longer spacer length correlates with the presence of flatter layers and that shorter spacer length (or the complete absence of spacers, as in our model microemulsion) correlates with the presence of layer curvature.

The resulting structure of potato starch can therefore be seen, using the model presented above, to suffer far more substantial distortions due to layer curvature than waxy maize but less than those of the microemulsion. This implies that the rigid mesogen units (i.e., amylopectin double helices) in potato starch are pulled out of register to a far higher degree than is the case for waxy maize, leading to a higher layer curvature (see Figure 3), though not as high a curvature as found in the microemulsion. Further evidence supporting the contrasting organization of potato starch granules, com-

pared with that of other species of starch granules, can be found in the experimental observations recently reported in refs 26−28 and 36−38.

The overall implication for starch granule structure[27] (and similar lamellar materials) is that, given enough freedom (via longer or more flexible spacers), the lamellae tend to arrange themselves into a well-aligned, flat-layered structure (although lateral discontinuities, as suggested by some microscopic evidence,[20] cannot be ruled out in the case of starch). If this is no longer possible (due to shorter or less flexible spacers), then initially the layers will tend to bend slightly, giving rise to weak lamellar splay distortions. Finally, when the layers have reached the maximum amount of splay distortion that they can tolerate, then the lamellae become much more "crumpled" with much greater layer bend and curvature (see Figure 3).

An intuitive explanation of the lamellar structure in our starch−water systems, compared to our microemulsion system, can be forged due to the smectic side-chain liquid-crystalline polymer properties of starch. The rigid, mesogenic amylopectin units are attached to an amorphous backbone via flexible spacers. When the flexible spacers are mobile enough (via longer length,[27,28] sufficient hydration or solvent,[17−19] or sufficient temperature[36]), the mesogenic units are able to arrange themselves side-by-side to form a smectic-type structure. Indeed, if the degree of mobility and entropy of the flexible spacers is sufficiently reduced, then it is found that the 9 nm peak observed in starch scattering disappears,[36] along with an associated endothermic DSC transition.[36] Also, it was found in refs 17−19 that the lamellar organization under plasticization of potato starch can take up to 5 times as long as waxy maize starch upon storage at room temperature. So, upon increasing the mobility of the flexible spacer units (and therefore adequately decoupling the mesogenic units from the amorphous backbone), starch can be seen to be able to self-assemble into an ordered smectic-like lamellar system. The resulting lamellar structure is strongly dependent on the starch cultivar, whose characteristics can now be quantitatively characterized for the first time using the completely general model outlined in this work.

Similar assembly considerations are well-known in other lamellar systems. For example, in amphiphilic systems (held together by hydrophobic/hydrophilic interactions), the geometry of the underlying surfactant units is crucial in determining which of a number of equilibrium macroscopic structures is assumed.[1,5] Also in side-chain liquid-crystalline polymers,[1,2,9−14] the combination of connectivity with that of flexibility (of the spacers) and rigidity (of the mesogens) leads to supramolecular assemblies qualitatively different from those of canonical smectic systems, where such connectivity constraints are absent.[1,2,5] Arising out of the work presented here, and within its associated biological setting, analogous considerations can now be seen to be highly relevant insofar as starch as a soft material is concerned.

What seems to be crucial in distinguishing the precise type of lamellar structure present in starch, or lamellar systems, that arises from this work, is the value of the coarse-grained, effective bending modulus.[27,34] This value of the bending modulus arises as a direct consequence of the structure and molecular packing involved in a particular material. Perhaps more tellingly is the exponential dependence of the correlation length ξ on the bending modulus. The well-known de Gennes−Taupin length[34] for fluctuating surfaces, ξ, is defined as the length scale up to which the layer normal vectors remain correlated. The correlation length ξ can typically be written as[27,34] $\xi = be^{\pi K/k_B T}$ (with a short distance cutoff b). Note how extremely sensitively the correlation length depends on the layer bending modulus K. Given this exponential dependence of the correlation length on the layer bending modulus, we can see that in the ideal flat limit $K \rightarrow \infty$ we must consistently take the correlation length to be very large also, which implies $\xi \rightarrow \infty$.[27,34]

Given such an exquisitely sensitive dependence of local layer flatness on the coarse-grained stiffness modulus (itself given by the fine-grained molecular structure), perhaps it is not surprising that such intermediate, lamellar behavior is observed[27] for starch granules, as shown in this work. Indeed, lessons learned from the lamellar structure of starch could well prove insightful in the novel design and synthesis of just such specifically intermediate, multilayered materials. Typically, lamellar material properties are experimentally probed and manipulated by directly altering the underlying spontaneous curvature of the layers and not by directly altering the bending modulus itself. Given what we have learned from the supramolecular assembly of starch in this work, and its effect on the coarse-grained bending modulus, K, novel materials designed along similar morphological lines as starch could well prove to be our best chance of exploring, manipulating, and exploiting this K dependence in the design of new materials.

Conclusion

In this work we have presented the soft matter, lamellar properties of starch and compared it with a model multilayered microemulsion system. We have learned how to characterize and quantify the degree of layer bending in soft lamellar materials, and how this behavior in starch can be correlated with flexible spacer length, supporting the conclusion that starch can be viewed successfully and usefully as a SSCLCP.

Given the above considerations, we can see that starch granules, in comparison with model microemulsions, are able to arrange themselves into a structure intermediate between that of an ideal, flat lamellar system and that associated with a canonical smectic system. The extent of this interesting material property of starch is species-dependent and results as a direct consequence of the combined effects of packing constraints, connectivity, and mobility of its constituent units (consistent with filling space and the material being laid down sequentially in time). Thus, it can be seen that the supramolecular packing present in starch granules is able to confer subtly different properties on its lamellar structure, over and above those found in canonical smectic materials, typified by our model microemulsion.

Allied to the above main point of this work, and worth emphasizing, is that the ideal, flat limit is never seen in the much studied, canonical lamellar systems, such as fluid membranes,[5−8,26−33] smectic liquid crystals,[1−4] and, as exemplified in this work, surfactant-based systems.[5,6] These systems are intrinsically characterized by the complete absence of long-range order and are dominated by transverse layer fluctuations. Starch, on

the other hand, can be seen to be able to arrange itself in such a way that its lamellar structure lies somewhere between that characterized by the presence of long-range order and the total absence of long-range order. This insight leads one to suspect that a broad wealth of such intermediate structural properties may indeed be lurking in similar lamellar materials.

Finally, we would like to emphasize the fascinating lamellar properties of starch as a biologically relevant form of self-assembling soft matter, viewed as a SSCLCP. Indeed, this work was partly motivated by a strong desire to introduce starch to the wider soft matter community. Valuable insights gleaned from the structure of starch could well prove to be extremely useful in the design and synthesis of new and novel lamellar materials with interesting properties. Furthermore, genetic engineering is rapidly making possible designer starches, for which the quantitative model presented in this work will prove invaluable in describing, characterizing, and understanding their lamellar (and hence processing) properties.

Acknowledgment. Many thanks to Eugene Terentjev for several helpful discussions and to DuPont (U.K.) Limited for their support. Many thanks also to Professor C. R. Safinya for his kind permission in allowing us to use the SAXS data points taken from ref 6.

References and Notes

(1) Chaikin, P. M.; Lubensky, T. C. *Principles of Condensed Matter Physics*; Cambridge University Press: New York, 2000.
(2) De Gennes, P. G. *The Physics of Liquid Crystals*; Clarendon Press: Oxford, 1974.
(3) Als-Nielsen, J.; Lister, J. D.; Birgeneau, R. J.; Kaplan, M.; Safinya, C. R.; Lindegaard-Andersen, A.; Mathiesen, S. *Phys. Rev. B* **1980**, *22*, 312−320.
(4) Kaganer, V. M.; Ostrovskii, B. I.; de Jeu, W. H. *Phys. Rev. A* **1991**, *44*, 8158−8166.
(5) Safran, S. A. *Statistical Thermodynamics of Surface, Interfaces and Membranes*; Addison-Wesley: Reading, MA, 1994.
(6) Safinya, C. R.; Roux, D.; Smith, G. S.; Sinha, S. K.; Dimon, P.; Clark, N. A.; Bellocq, A. M. *Phys. Rev. Lett.* **1986**, *57*, 2718−2721.
(7) Lei, N.; Safinya, C. R.; Bruinsma, R. F. *J. Phys. II* **1995**, *5*, 1155−1163.
(8) Nallet, F.; Laversanne, R.; Roux, D. *J. Phys. II* **1993**, *3*, 487−502.
(9) Warner, M. In *Side Chain Liquid Crystal Polymers*; Blackie: Glasgow, 1989.
(10) Simmonds, D. In *Liquid Crystal Polymers*; Elsevier: London, 1992.
(11) Rieger, J. *Liq. Cryst.* **1989**, *5*, 1559−1565.
(12) Warner, M. *Philos. Trans. R. Soc. London A* **1993**, *344*, 403−417.
(13) Wang, X. J.; Warner, M. *Liq. Cryst.* **1992**, *12*, 385−401.
(14) Warner, M. *Mol. Cryst. Liq. Cryst.* **1988**, *155*, 433−442.
(15) Boal, D. *Mechanics of the Cell*; Cambridge University Press: New York, 2001.
(16) Cameron, R. E.; Donald, A. M. *Polymer* **1992**, *33*, 2628−2635.
(17) Waigh, T. A.; Perry, P.; Riekel, C.; Gidley, M. J.; Donald, A. M. *Macromolecules* **1998**, *31*, 7980−7984.
(18) Waigh, T. A.; Donald, A. M.; Heidelbach, F.; Riekel, C.; Gidley, M. J. *Biopolymers* **1999**, *49*, 91−105.
(19) Waigh, T. A.; Kato, K. L.; Donald, A. M.; Gidley, M. J.; Clarke, C. J.; Riekel, C. *Starch/Starke* **2000**, *52*, 450−460.
(20) Gallant, D. J.; Bouchet, B.; Baldwin, P. M. *Carbohydr. Polym.* **1997**, *32*, 177−191.
(21) Blanshard, J. M. V.; Bates, D. R.; Muhr, A. H.; Worcester, D. L.; Higgins, J. S. *Carbohydr. Polym.* **1984**, *4*, 427−442.
(22) Oostergetel, G. T.; Vanbruggen, E. F. J. *Carbohydr. Polym.* **1993**, *21*, 7−12.
(23) Oostergetel, G. T.; et al. *Food Hydrocolloids* **1987**, *1*, 527−528.
(24) Oostergetel, G. T.; et al. In *Proceedings of the 13th Electron Microscopy Meeting in Paris*, 1994; pp 535−537.
(25) Oostergetel, G. T.; Vanbruggen, E. F. J. *Starch* **1989**, *41*, 331−335.
(26) Hizukuri, S. *Carbohydr. Res.* **1985**, *141*, 295−306.
(27) Daniels, D. R.; Donald, A. M. *Biopolymers* **2003**, *69*, 165−175.
(28) Sanderson, J. S. Physical Aspects of Starch Biodiversity. Ph.D. Thesis, University of Cambridge, 2003.
(29) Helfrich, W. *Z. Naturforsch.* **1973**, *28C*, 693−699.
(30) Helfrich, W. *Z. Naturforsch.* **1978**, *33A*, 305−315.
(31) Zhang, R.; Suter, R. M.; Nagle, J. F. *Phys. Rev. E* **1994**, *50*, 5047−5060.
(32) Zhang, R.; Tristram-Nagle, S.; Sun, W.; Headrick, R. L.; Irving, T. C.; Suter, R. M.; Nagle, J. F. *Biophys. J.* **1996**, *70*, 349−357.
(33) Caille, A. *A. C. R. Acad. Sci. Paris* **1972**, *274B*, 891−893.
(34) De Gennes, P. G.; Taupin, C. *J. Phys. Chem.* **1982**, *86*, 2294−2304.
(35) Hosemann, R.; Bagchi, S. N. *Direct Analysis of Diffraction by Matter*; North Holland: Amsterdam, 1962.
(36) Waigh, T. A. The Structure and Side-Chain Liquid Crystalline Polymeric Properties of Starch. Ph.D. Thesis, University of Cambridge, 1997.
(37) Pilling, E. The Origins of Growth Rings in Starch Granules. Ph.D. Thesis, University of East Anglia, 2001.
(38) Fulton, D. C.; et al. *J. Biol. Chem.* **2002**, *277*, 10834−10841.

MA030360H